# Shock-front broadening in polycrystalline materials

J. L. Barber* and K. Kadau
*Los Alamos National Laboratory, Los Alamos, New Mexico 87545, USA*
(Received 18 December 2007; published 9 April 2008)

We analyze a model for the evolution of shock fronts in polycrystalline materials. This model is based on the idea of Meyers and Carvalho [Mater. Sci. Eng. **24**, 131 (1976)] that the shock velocity anisotropy within the polycrystal is the most important factor in shock front broadening. Our analysis predicts that the shock front width increases as the 1/2 power of the front penetration distance into the crystal. Our theoretical prediction is in plausible agreement with previous experimental results for the elastic precursor rise time, and it should therefore provide a useful shock width estimate. Furthermore, our theoretical framework is also applicable to other problems involving front propagation in heterogeneous media.

DOI: 10.1103/PhysRevB.77.144106 PACS number(s): 62.50.Ef, 47.40.Nm

It has been observed experimentally that a shock front propagating through a polycrystalline solid, in which each grain has a different crystallographic orientation of the same material, will increase in width over time.[1,2] This broadening has a significant effect on the postshocked state of the material,[3] and may occur via a number of mechanisms, including scattering at grain boundaries, and, in strong shocks, plasticity effects. Meyers and Carvalho[4,5] proposed a model in which the sole contributor to front broadening in elastic shocks is the shock speed anisotropy between differently oriented grains within the polycrystal. This anisotropy causes different regions of the shock front to propagate at different speeds.

This model was originally studied via simulations using a very simplified representation of a polycrystal.[4,5] In this work, we trace the mathematical consequences of the model for a more realistic polycrystalline topology and provide a shock width estimate for a wide variety of materials. After an outline of the assumptions of the model, we perform a probabilistic analysis of the resulting dynamics, followed by a comparison of our theoretical predictions with simulations of the model itself and with experimental data from the literature.

Suppose that the polycrystal occupies a $D$-dimensional domain, where $D$ is kept arbitrary for generality. We define the $+x$ axis as the direction of shock propagation and collectively label all transverse coordinates as $y$ (see Fig. 1). The initially flat front starts at $x=0$, and each point on the shock front propagates into the bulk of the solid independently, with a velocity in the $+x$ direction. This generates a set of distinct rays, distinguished by their transverse coordinates $y$.

The propagation speed along an arbitrary ray is given by the function $v(x,y)$, the statistics of which depends on the distribution of shock speeds and the geometry of the grains. Suppressing $y$ dependence for conciseness, the time required for a point on the shock front to reach $x$ is

$$t = \int_0^x dx' \frac{1}{v(x')} = \frac{x}{c} + \int_0^x dx' \left( \frac{1}{v(x')} - \frac{1}{c} \right), \tag{1}$$

where $1/c = \langle 1/v \rangle$ is the mean inverse shock speed. Here, $\langle \ldots \rangle$ represents an average over both the distribution of shock speeds and the stochastic geometry of the grains. The integrand $1/v(x') - 1/c$ in Eq. (1) is a mean-zero random field. We define its spatial correlation function as $\chi(x,x') \equiv \langle [1/v(x) - 1/c][1/v(x') - 1/c] \rangle$.

Our two major assumptions are statistical isotropy and that the shock speeds in different grains are independent. The former implies that $\chi(x,x') = \chi(|x-x'|)$, whereas the latter implies that $\chi(x) \geqslant 0$ for all $x$. If, in addition, the grains are convex (as in a Voronoi lattice), then $\chi(x)$ will be monotonically decreasing in $x$. Under these assumptions, it can be proven[6] that for large $x$ the integral in Eq. (1) converges in distribution to

$$\int_0^x dx' \left( \frac{1}{v(x')} - \frac{1}{c} \right) \to \left( 2x \int_0^\infty dx' \chi(x') \right)^{1/2} \mathbb{Z}, \tag{2}$$

where $\mathbb{Z}$ is a standard normal random variable. In the large-$x$ limit, Eq. (1) can therefore be written as

$$ct = x + (2a)^{1/2} x^{1/2} \mathbb{Z}, \tag{3}$$

where $a \equiv c^2 \int_0^\infty dx \chi(x)$ has units of length. Equation (3) can be inverted to obtain the random $x$ coordinate of a point on the shock front as a function of $t$,

$$x = ct + a\mathbb{Z}^2 + (a/2)^{1/2} \mathbb{Z} \sqrt{2a\mathbb{Z}^2 + 4ct}. \tag{4}$$

We define the average shock front position and shock front width as $\bar{x} \equiv \langle x \rangle$ and $\Delta x \equiv 2\langle (x-\bar{x})^2 \rangle^{1/2}$, respectively. From Eq. (4), it follows that, to leading order in $t$, these are

$$\bar{x} = ct, \tag{5}$$

$$\Delta x = (8act)^{1/2}. \tag{6}$$

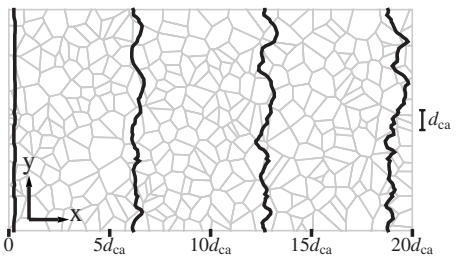


FIG. 1. Schematic representation of the polycrystal, with several shock front profiles from a 2D model simulation.

 

In order to render these expressions scale invariant, $\bar{x}$ and $\Delta x$ should be expressed in terms of the average grain size, of which several definitions exist. In experimental work, a sectional diameter $d_{\text{sec}}$ is often used, defined as the diameter of a circle of area equal to the average area of sectional grains in a cross section of the polycrystal. Also in use experimentally is the mean chord length $d_{ch}$, defined as the mean length of chords generated by the intersections between grain boundaries and a random line. In this work, we use the mean caliper length $d_{ca}$ from stochastic geometry, which is defined as the mean length of a grain's projection onto a random line.[13]

Eliminating $t$ between Eqs. (5) and (6) and dividing both sides by $d_{ca}$ yields the relation

$$\frac{\Delta x}{d_{ca}} = A\left(\frac{\bar{x}}{d_{ca}}\right)^{1/2}, \tag{7}$$

which is scale invariant in the grain size, and where

$$A \equiv \left(\frac{8c^2}{d_{ca}}\int_0^\infty dx\chi(x)\right)^{1/2} \tag{8}$$

is the dimensionless anisotropy coefficient. Equations (7) and (8) are the most general results of this work. Note that Eq. (7) is consistent with a power-law fit to molecular dynamics (MD) simulation data,[7] which found $\Delta x/d_{ca} \propto d_{ca}^{\alpha}$, with $\alpha \sim -1/2$.

In order to simplify the determination of the anisotropy coefficient, we make the additional assumption that each grain's shock speed is statistically independent of the grain geometry. Then, $\chi$ decomposes as

$$\chi(x) = \chi_o \psi_D(x), \tag{9}$$

where $\chi_o \equiv \langle (1/v - 1/c)^2 \rangle$ and $\psi_D(x)$ is the probability that two points in the $D$-dimensional polycrystal a distance $x$ apart fall within the same grain. It can be shown[6] that

$$\int_0^\infty dx\psi_D(x) = \frac{d_{ch}}{2}\left(1 + \frac{\sigma_{ch}^2}{d_{ch}^2}\right), \tag{10}$$

where $\sigma_{ch}$ is the standard deviation of the intersectional chord lengths mentioned in the definition of $d_{ch}$. For a three-dimensional (3D) [two-dimensional (2D)] Poisson–Voronoi lattice (PVL), $\sigma_{ch} = 0.400n^{-1/3}$ $[0.433n^{-1/2}]$. Given Eqs. (9) and (10), the anisotropy coefficient becomes

$$A = \left[4c^2\chi_o \frac{d_{ch}}{d_{ca}}\left(1 + \frac{\sigma_{ch}^2}{d_{ch}^2}\right)\right]^{1/2}. \tag{11}$$

In addition to an expression for the front broadening $\Delta x$, this model also predicts the correlation in the shock front position $x(y,t)$ in the direction $y$ lateral to the shock front. Restoring the explicit $y$ dependence, we define the shock front correlation function as

$$C(|y - y'|, t) \equiv \frac{\langle [x(y,t) - \bar{x}(t)][x(y',t) - \bar{x}(t)] \rangle}{[\Delta x(t)/2]^2}. \tag{12}$$

It can be shown[6] that for large $t$,

$$C(y,t) \to \phi_D(y) \equiv \frac{\int_0^\infty dy' \chi(\sqrt{y'^2 + y^2})}{\int_0^\infty dy' \chi(y')}. \tag{13}$$

Equations (7), (8), (11), and (13) are predictions for large $t$. We can also derive expressions for the behavior of the shock front in the limit of small $t$. In this limit, the penetration distance of ray $y$ at time $t$ is given approximately by $x(y,t) = v(y)t$, where $v(y)$ is the shock speed profile at $y = 0$. From this, it follows that

$$\frac{dx}{d_{ca}} = \frac{2\sigma_v}{\bar{v}}\frac{\bar{x}}{d_{ca}}, \tag{14}$$

where $\bar{v}$ and $\sigma_v$ are, respectively, the mean and standard deviation of the distribution of shock speeds within each grain. Furthermore, for small $t$, the shock front correlation function $C(y,t)$ will be identical to $\psi_D(y)$, since $v(y)$ correlates in the same way as grain membership.

It should be noted that, in practice, there is some ambiguity in the meaning of the average $\langle \cdots \rangle$, which is used for calculating $c$, $\chi_o$, and $A$. We make use of two different interpretations of this average, which we call "average 1" and "average 2."

*Average 1*. In Refs. 4 and 5, it is noted that for a crystal with cubic symmetry, 100, 110, and 111 are the only directions in which purely longitudinal acoustic waves are possible. These move with speeds $u_{100}$, $u_{110}$, and $u_{111}$, respectively. In this average, we consider only the shock speeds in these three directions, which are given probabilities proportional to their multiplicity factors (6, 12, and 8, respectively). We obtain estimates for these three shock speeds in two ways. First, in the 3D acoustic—or weak shock—limit via the expressions $u_{100} = \sqrt{C_{11}/\rho}$, $u_{110} = \sqrt{(C_{11} + C_{12} + 2C_{44})/\rho}$, and $u_{111} = \sqrt{(C_{11} + 2C_{12} + 4C_{44})/\rho}$, where the $C$ are the elastic stiffnesses of the material and $\rho$ is the mass density.[4] Second, for moderate shock strengths, from the plateau elastic precursor wave speeds in single-crystalline MD simulations of Fe in Ref. 8.

*Average 2*. In reality, the orientation of grains within a polycrystal is not solely restricted to the three mentioned above. For an arbitrary orientation, one can use the elastic equations for the propagation of acoustic waves in an inhomogeneous medium to find the shock speed $u(\Omega)$ in an arbitrary direction.[6] By assuming that grain orientations are uniformly distributed on the unit sphere, we can calculate $c$, $\chi_o$, and $A$.

The values of $c$, $\chi_o$, and $A$ calculated using the acoustic properties of several materials via each of these two averages are given in Table I. Note that the calculation of $A$ assumes a PVL.

In order to verify the steps leading to the theoretical predictions above, we have performed several direct simulations of the model itself. A 2D PVL was generated by selecting a number of grain centers randomly and uniformly throughout a rectangular domain. The shock front speed within each grain was randomly selected as one of three velocities, with

TABLE I. Calculated properties of various materials.

| | Average 1 (Acoustic) | | | Average 2 | | |
|---|---|---|---|---|---|---|
| | $c$ $(\frac{\mathrm{m}}{\mathrm{s}})$ | $\chi_0$ $(10^{-11}\ \frac{\mathrm{s}^2}{\mathrm{m}^2})$ | $A$ | $c$ $(\frac{\mathrm{m}}{\mathrm{s}})$ | $\chi_0$ $(10^{-11}\ \frac{\mathrm{s}^2}{\mathrm{m}^2})$ | $A$ |
| Fe[a] | 6180 | 10.3 | 0.0998 | 6190 | 4.13 | 0.0632 |
| W | 5210 | 0.00141 | 0.000982 | 5210 | 0.000690 | 0.000688 |
| Ta | 4140 | 4.31 | 0.0432 | 4130 | 1.97 | 0.0292 |
| Cu | 4840 | 19.3 | 0.107 | 4840 | 7.70 | 0.0776 |
| Ag | 3750 | 22.0 | 0.0885 | 3750 | 9.22 | 0.0572 |
| Au | 3330 | 9.99 | 0.0528 | 3320 | 4.52 | 0.0354 |
| Al | 6380 | 0.339 | 0.0186 | 6370 | 0.162 | 0.0129 |
| K | 2370 | 145 | 0.143 | 2380 | 52.9 | 0.0870 |
| Pb | 2250 | 52.0 | 0.0816 | 2250 | 22.2 | 0.0534 |
| Ni | 5890 | 11.8 | 0.102 | 5890 | 4.71 | 0.0642 |
| Pd | 4680 | 9.76 | 0.0735 | 4670 | 4.23 | 0.0482 |

[a]For Fe, the plateau elastic precursor speeds given in Ref. 8 yield $c=6120$ m/s, $\chi_0=20.3\times10^{-11}$ s$^2$/m$^2$, and $A=0.138$ for average 1 (MD).

weights 6, 12, and 8, as described above. Other than the anisotropy coefficient, which was 0.153, the precise numbers used are of little importance, since the expressions we have derived are scale invariant. A number of points on the shock front starting at $x=0$ were propagated in the $+x$ direction according to this random velocity field. Some representative front profiles at various penetration depths from a small $20\times10$ grain simulation are shown in Fig. 1. In order to improve the statistics to allow comparison with our predictions, we also performed a larger $20\times2560$ grain simulation. Results for $\Delta x/d_{ca}$ vs $\bar{x}/d_{ca}$, as well as for $C(y)$ are compared to the theory in Fig. 2. The shock width obeys Eq. (7) nearly perfectly at late times and (although it is difficult to discern in the figure) Eq. (14) at early times. Also, as predicted, $C(y,t)$ agrees with $\phi_{2\mathrm{D}}(y)$ for large $t$ and $\psi_{2\mathrm{D}}(y)$ for small $t$.

These numerical simulations validate our mathematical results and provide some insight into the dynamics of the model. Of greater importance, however, is a comparison between our theoretical predictions and experimental data from the literature. The two experimental papers we considered were Arvidsson *et al.*[1] and Jones and Holland,[2] which used samples of polycrystalline aluminum and steel, respectively.

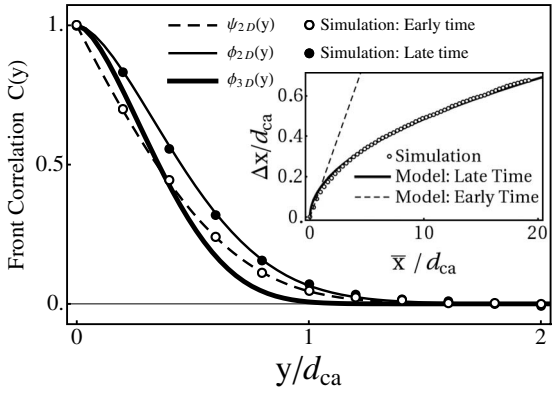


FIG. 2. Front correlation $C(y)$ generated by direct simulation of the model on a 2D PVL, compared to our early, and late-time theories. [$\phi_{3\mathrm{D}}(y)$ is shown for reference.] Inset: $\Delta x/d_{ca}$ vs $\bar{x}/d_{ca}$ from the same simulation, compared to theory.

There were a number of difficulties in interpreting the experimental data, which allowed only a rough comparison between theory and experiment. The data are given in terms of rise times for the elastic precursor wave. The elastic wave speed, which was needed in order to translate these into shock widths, was given in Ref. 2 as 5857 m/s, but it was omitted in Ref. 1 As a rough estimate, we used 6400 m/s, the longitudinal sound speed of Al. We assumed a PVL geometry for all samples. From the values of $d_{ch}$ reported in Ref. 2, this allowed us to infer that their $d_{ca}$ values varied between 19.1 and 149 $\mu$m. In Ref. 1, $d_{ca}=284$ $\mu$m.[14]

Finally, in both Refs. 1 and 2, the rise time is measured as the time interval between minimum and maximum stresses at the sample surface, whereas our two-standard-deviation definition for the shock width implies that we should instead compare to the interval around the median stress which contains 68.3% of this variation. A graphical analysis of the stress-time profiles in Ref. 2 indicates that this can be obtained by multiplying the reported rise times by ~0.4. We have adjusted both data sets accordingly.

Comparisons between our theory and the data of Ref. 1 and 2 are shown in Figs. 3 and 4, respectively. Despite many approximations, including the neglect of grain boundary effects, there is good consistency between theory and experiment. Shown are the theoretical predictions corresponding to both average 1 and average 2 using acoustic data. Also shown are curves corresponding to average 1 using MD data. The $A$ used in these curves were derived from the data in Ref. 8 Although these data were obtained from simulated Fe, the Hugoniot curves of Fe and steel are similar for weak shocks,[9] and it was therefore reasonable to use the resulting $A$ value with the data of Jones and Holland. Lacking single-crystal shock speeds for Al, the value of $A$ (average 1, MD) used in Fig. 3 was arrived at by assuming that the ratio of $A$

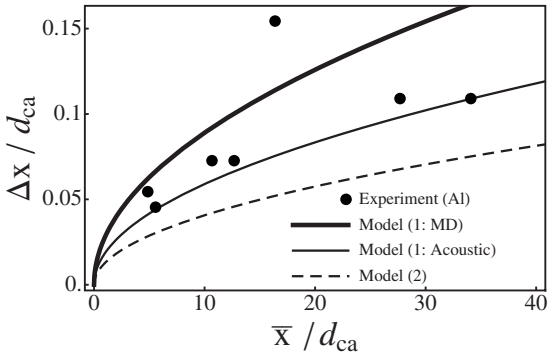


FIG. 3. Comparison of the Al data by Arvidsson *et al.* with our model for each of the three ways of calculating the averages.

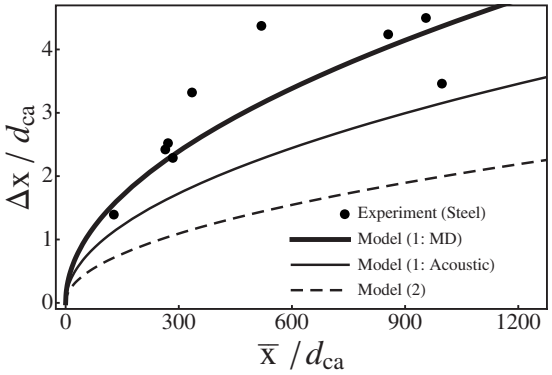


FIG. 4. Comparison of the steel data of Jones and Holland with our model for each of three ways of calculating the averages.

(average 1, MD) to $A$ (average 1, acoustic) was the same in Fe and Al.

These results suggest that the analytical theory presented here successfully describes shock front broadening, yielding plausible agreement with experimental data, and should provide a useful estimate of shock front widths for various materials. In cases where a split two-wave structure is present, this theory applies to the elastic and plastic waves separately. Note that, in addition to grain boundary effects, this model also neglects shear forces that may reduce the independence between different regions of the shock front, thereby decreasing the shock width. This effect may become more pronounced as the front width increases. An interesting avenue of future work would be the more difficult problem of incorporating grain boundary effects into this model, which could then be compared to MD simulation data for nanocrystalline materials. This would allow for a quantitative estimate of the importance of nonscale-invariant effects due to grain boundaries, which are proportionally larger at the scales currently accessible to MD. Lastly, the theoretical framework given in this work is not specific to shock fronts in polycrystals and may have other applications to front propagation problems in which anisotropy and heterogeneity are important factors.

## ACKNOWLEDGMENTS

We would like to thank N. Park, R. J. Ravelo, C. M. Newman, J. Møller, Y. Gupta, P. Trivedi, T. C. Germann, B. L. Holian, and E. M. Kober for valuable input. This work was carried out under the auspices of the National Nuclear Security Administration of the U.S. Department of Energy at Los Alamos National Laboratory under Contract No. DE-AC52-06NA25396, with funding by ASC.

*jlbarber@lanl.gov

[1] T. Arvidsson, Y. Gupta, and G. Duvall, J. Appl. Phys. **46**, 4474 (1976).
[2] O. Jones and J. Holland, Acta Metall. **16**, 1037 (1968).
[3] K. T. Gahagan, D. S. Moore, D. J. Funk, R. L. Rabie, S. J. Buelow, and J. W. Nicholson, Phys. Rev. Lett. **85**, 3205 (2000).
[4] M. A. Meyers and M. S. Carvalho, Mater. Sci. Eng. **24**, 131 (1976).
[5] M. A. Meyers, Mater. Sci. Eng. **30**, 99 (1977).
[6] See EPAPS Document No. E-PRBMDO-77-031814 for proofs, derivations, and explanations of various mathematical points raised in the main text. For more information on EPAPS, see http://www.aip.org.pubservs/epaps.html
[7] E. M. Bringa, A. Caro, M. Victoria, and N. Park, JOM **57**, 67 (2005).
[8] K. Kadau, T. C. Germann, P. S. Lomdahl, and B. L. Holian, Phys. Rev. B **72**, 064120 (2005).
[9] N. Bourne and J. Millett, Scr. Mater. **43**, 541 (2000).
[10] A. Okabe, B. Boots, and K. Sugihara, *Spatial Tesselations: Concepts and Applications of Voronoi Diagrams* (Wiley, New York, 1992).
[11] Y. Gupta and P. Trivedi (private communication).
[12] X. Chen, J. Asay, and S. Dwivedi, J. Appl. Phys. **99**, 023528 (2006).
[13] For a 3D PVL, $d_{sec}=0.935n^{-1/3}$, $d_{ch}=0.687n^{-1/3}$, and $d_{ca}=1.458n^{-1/3}$, where $n$ is the number density of grains (Ref. 10). In 2D, $d_{ch}=0.785n^{-1/2}$ and $d_{ca}=1.273n^{-1/2}$.
[14] The grain size in Ref. 1 is apparently a typo (Ref. 11). The value of $d_{sec}$ given in Ref. 12 implies that $d_{ca}=284$ $\mu$m for the same type of Al.